

# Options for using Landsat and RapidEye satellite images aiming the water productivity assessments in mixed agro-ecosystems

Antônio H. de C. Teixeira<sup>\*a</sup>, Janice F. Leivas<sup>a</sup>, Gustavo Bayma-Silva<sup>a</sup>

<sup>a</sup>Embrapa Satellite Monitoring, Campinas, São Paulo, Brazil.

## ABSTRACT

For water productivity (WP) assessments, the SAFER (Surface Algorithm for Evapotranspiration Retrieving) algorithm for evapotranspiration (ET) and the Monteith's light use efficiency (LUE) model for biomass production (BIO), were applied to Landsat and RapidEye satellite images, in the Brazilian semiarid region, inside the dry season of 2011, in a mixture of irrigated and rainfed agro-ecosystems. Firstly, with the Landsat image, the methodology from which the surface temperature ( $T_0$ ) is derived as a residue in the radiation balance was tested. Low differences were detected, being Landsat ET with the thermal band averaged  $0.9 \pm 1.5 \text{ mm d}^{-1}$ , while without it the mean value was  $0.8 \pm 1.5 \text{ mm d}^{-1}$ . The corresponding Landsat BIO values were respectively  $28 \pm 59$  and  $28 \pm 58 \text{ kg ha}^{-1} \text{ d}^{-1}$ , resulting in mean WP of  $1.3 \pm 1.3 \text{ kg m}^{-3}$ , in both cases. After having confidence on the residual methodology for retrieving  $T_0$  it was applied to the RapidEye image, resulting in average pixel values for ET, BIO and WP of  $0.6 \pm 1.5 \text{ mm d}^{-1}$ ,  $26 \pm 58 \text{ kg ha}^{-1} \text{ d}^{-1}$  and  $0.9 \pm 1.3 \text{ kg m}^{-3}$ , representing 75%, 93% and 69% of the Landsat ones obtained without the thermal band. In addition, the Surface Resistance Algorithm (SURREAL) was used to classify the agro-ecosystems into irrigated crops and natural vegetation by using the RapidEye image. The incremental values for ET, BIO and WP in 2011 were  $2.0 \pm 1.3 \text{ mm d}^{-1}$ ,  $88 \pm 87 \text{ kg ha d}^{-1}$  and  $2.5 \pm 0.6 \text{ kg m}^{-3}$ , respectively, as a result of the replacement of the natural species by crops.

**Keywords:** remote sensing, evapotranspiration, biomass production, agrometeorological stations.

## 1. INTRODUCTION

For large scale hydrological modeling it is important that evapotranspiration (ET) and biomass production (BIO) to be acquired at good both spatial and temporal resolutions to incorporate the water and vegetation dynamics in environmental studies. These biophysical parameters are very variable in relation to the large-scale of precipitation and irrigation water and according to the different agro-ecosystems<sup>1</sup>. The difficult of estimating ET and BIO in mixed ecosystems throughout field measurements highlighted remote sensing by satellite images as a strong tool, which has been used in studies involving different climate conditions and varying spatial resolutions<sup>2-3</sup>.

To use satellite images for determining ET and BIO on large scales, in general the thermal band is required in some algorithms to retrieve the surface temperature ( $T_0$ ) and it is absent in some high temporal resolution satellites, giving some limitations for environmental studies. To overcome this problem, downscaling and interpolation techniques have been developed and applied<sup>4</sup>.

The RapidEye sensor does not have a thermal band, but with a good spatial resolution of 5 m, provides images of large cover areas, at frequent revisits and multispectral capabilities. There is a constellation of five satellites with identical sensors in the same orbital plan and equally calibrated among them.

The objective of the actual research was to test and apply a new methodology of assessing Water Productivity (WP) being  $T_0$  retrieved with and without the thermal band of the Landsat sensor and later apply it to the RapidEye image, to see the suitability of this last satellite for WP assessments in mixed agro-ecosystems. WP is considering the ratio of ET

---

<sup>\*</sup>heriberto.teixeira@embrapa.br; Phone 55 19 3211-6200; Fax: 55 19 3211-6222; www.cnpm.embrapa.br

to BIO, with the first parameter determined by the SAFER (Simple Algorithm for Evapotranspiration Retrieving) algorithm and BIO estimated by the Monteith's Light Use Efficiency (LUE)<sup>3</sup>. An area inside the semi-arid region of the Northeast Brazil is taken as a reference, as this region has experienced fast land use changes, with irrigated crops replacing the natural species from the natural rainged vegetation called "Caatinga".

## 2. MATERIAL AND METHODS

### 2.1. Study area and data set

Fig. 1 shows the location of the semi-arid study area inside the Petrolina municipality, west side of the Pernambuco (PE) state, Northeast of Brazil, together with a net of four agrometeorological stations used for the weather data interpolation processes.

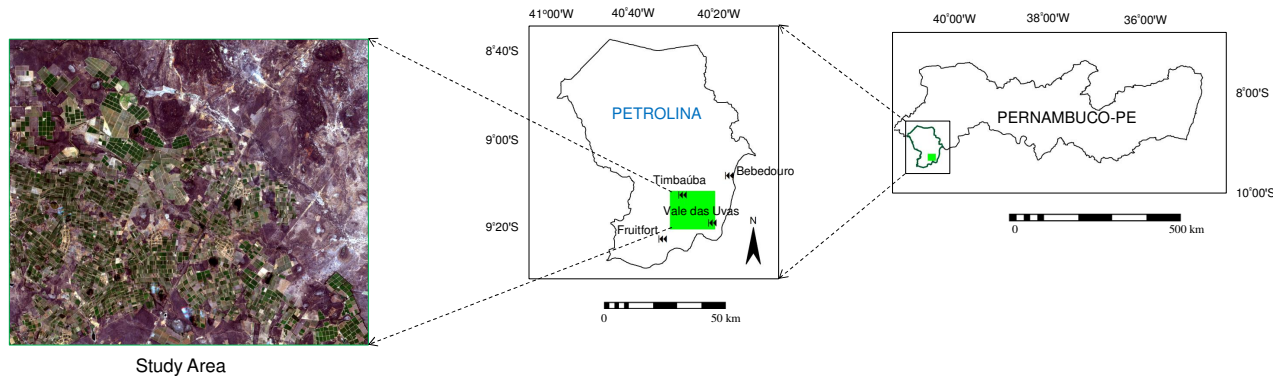


Figure 1. Location of the semi-arid study area inside the Petrolina municipality, west side of the Pernambuco (PE) state, Northeast Brazil, and the agrometeorological stations used for the weather data interpolation processes.

The study area present long-term annual air temperature ( $T_a$ ) higher than 24 °C, the average maximum value is 33 °C and its minimum is 19 °C. The warmest months are October and November when the sun at the zenith position with low cloud cover while the coldest ones are June and July at the winter solstice in the South hemisphere. Most rains fall during the first four months of the year, accounting for 68% of the total annual, which presents a long-term (50 years) of 570 mm yr<sup>-1</sup> registered at the Bebedouro agrometeorological station (see Fig. 1)<sup>3</sup>.

Mainly fruit crops compose the irrigated agro-ecosystems showed in Fig. 1 with a greener colour, being the main ones grapes for table and for juice, mangos, guava and bananas, surrounded by the natural vegetation called "Caatinga", represented by the browner colour. Data from four agrometeorological stations were used together with the Landsat 5 and RapidEye images acquired during the climatically driest conditions of the year 2011 (respectively Days of the Years - DOY: 240, August 29; and 253, September 10). Grids of global solar radiation ( $R_G$ ),  $T_a$  and reference evapotranspiration ( $ET_0$ ) were used together with the remotely sensed retrieved parameters during the steps of the large-scale WP modelling<sup>3</sup>.

### 2.2. Large-scale water productivity modelling

For modelling the WP components with and/or without the thermal bands, the SAFER (Simple Algorithm for Evapotranspiration Retrieving) algorithm was applied together with the Monteith's Light Use Efficiency (LUE) model. The remote sensing input parameters were surface albedo ( $\alpha_0$ ), surface temperature ( $T_0$ ) and the Normalized Difference Vegetation Index (NDVI). The equations are described in details in Teixeira et al.<sup>3</sup> being bellow summarized:

For both, Landsat and RapidEye images,  $\alpha_0$  was obtained from the planetary albedo for each satellite band ( $\alpha_{pb}$ ):

$$\alpha p_b = \frac{L_b \pi d^2}{R_{a_b} \cos \varphi} \quad (1)$$

where  $L_b$  is the spectral radiance for the wavelengths of the band b ( $\text{W m}^{-2} \text{ sr}^{-1} \mu\text{m}^{-1}$ ),  $d$  is the relative earth-sun distance;  $R_{a_b}$  is the mean solar irradiance at the top of the atmosphere for each band ( $\text{W m}^{-2} \mu\text{m}^{-1}$ ) and  $\varphi$  the solar zenith angle.

The broadband  $\alpha_p$  was calculated as the total sum of the different narrow-band  $\alpha p_b$  values according to the weights for each band ( $w_b$ ).

$$\alpha p = \sum w_b \alpha p_b \quad (2)$$

where  $\alpha p_b$  are from the bands 1 to 5 for RapidEye and 1 to 7 for Landsat.

By using the thermal region from the Landsat sensor, the spectral radiance from the band 6 ( $L_6$ ) was converted into radiometric temperatures applicable at the top of the atmosphere ( $T_b$ ):

$$T_b = \frac{K_2}{\ln(\frac{K_1}{L_6 + 1})} \quad (3)$$

where  $K_1$  and  $K_2$  are conversion coefficients.

The results for the instantaneous  $\alpha_p$  and  $T_b$  values were corrected atmospherically for acquiring the surface albedo ( $\alpha_0$ ) and surface temperature ( $T_0$ ), by regression equations resulted from instantaneous field and satellite measurements in the study region.

By applying the residual method, the 24-hour  $T_0$  values were estimated as:

$$T_0 = \sqrt[4]{\frac{R_G - \alpha_0 R_G + \epsilon_A \sigma T_a^4 - R_n}{\epsilon_S \sigma}} \quad (4)$$

where  $R_n$  is the net radiation at daily scale;  $\epsilon_A$  and  $\epsilon_S$  are respectively the atmospheric and surface emissivities; and  $\sigma$  is the Stefan-Boltzmann constant ( $5.67 \times 10^{-8} \text{ W m}^{-2} \text{ K}^{-4}$ ).

Daily  $R_n$  was estimated by using the Slob equation:

$$R_n = (1 - \alpha_0) R_G - a_L \tau_{sw} \quad (5)$$

where  $\tau_{sw}$  is the short-wave atmospheric transmissivity and the regression coefficient  $a_L$  was spatially distributed through its relationship with  $T_a$ .

With the SAFER algorithm, the ratio of actual (ET) to the reference ( $ET_0$ ) evapotranspiration -  $ET_r$ , was modelled at the satellite overpass time:

$$ET_r = \exp \left[ a_{sf} + b_{sf} \left( \frac{T_0}{\alpha_0 NDVI} \right) \right] \quad (6)$$

where  $ET_0$  was calculated by Penman-Monteith's method<sup>5</sup>, and  $a_{sf}$  and  $b_{sf}$  are the regression coefficients 1.8 and -0.008, respectively, for the Brazilian semi-arid conditions.

The  $ET_0$  daily grids from the agrometeorological station (black arrows on Fig. 1) were multiplied by the images resulted from Eq. 6, giving the large-scale daily ET pixel values:

$$ET = ET_r ET_0 \quad (7)$$

The biomass production (BIO) was quantified as:

$$BIO = \varepsilon_{max} ET_r APAR \cdot 0.864 \quad (8)$$

where  $\varepsilon_{max}$  is the maximum light use efficiency, APAR is the fraction of absorbed photosynthetically active radiation, and 0.864 is a conversion factor.

The water productivity (WP) was considered as:

$$WP = BIO/ET \quad (9)$$

For classification of the vegetated surface into irrigated crops and natural vegetation, the SUREAL (Surface Resistance Algorithm)<sup>6</sup> model was applied:

$$r_s = \exp \left[ a_r \left( \frac{T_0}{\alpha_0} \right) (1 - NDVI) + b_r \right] \quad (10)$$

where  $a_r$  and  $b_r$  are regression coefficients, considered respectively 0.04 e 2.72 for the Brazilian Northeast conditions. Pixels with  $r_s$  values below 800  $s m^{-1}$  and NDVI above zero were considered as irrigated crops. If  $r_s$  was in between 1,000 and 10,000  $s m^{-1}$ , the ecosystem should be natural vegetation.

### 3. RESULTS AND DISCUSSION

#### 3.1 Weather conditions

The weather-driving forces for WP are  $R_G$ ,  $T_a$ , precipitation (P), and the atmospheric demand represented by  $ET_0$ . These parameters are presented on a daily time-scale, during the year 2011, involving the previous, actual and post thermohydrological conditions for the satellite image acquisitions dates in August and September. Fig. 2 shows their trends in terms of Day of the Year (DOY), with weather data from the Timbaúba agrometeorological station (see Fig. 1).

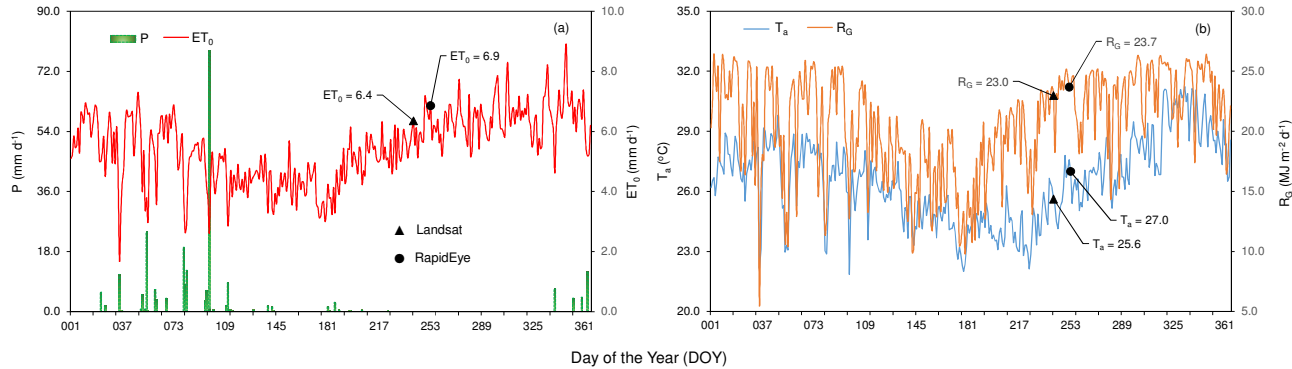


Figure 2. Daily values of the weather variables in terms of Day of the Year - DOY, for Landsat (DOY 241) and RapidEye (DOY 253) during 2011, in the semi-arid study area of the Petrolina municipality, Brazilian Northeast region. (a) Precipitation (P) and reference evapotranspiration ( $ET_0$ ). (b) incident global solar radiation ( $R_G$ ) and air temperature ( $T_a$ ).

P was the most variable weather parameter along the year with the highest values happening during the first four months, but inside the climatically driest period, at the days of image acquisitions there was absence of rains. Considering the  $ET_0$  values, one can see two peaks with the smallest ones happening at the middle of the year. However, when the values increased toward the end of the year, there was a small difference between the days of image acquisitions, with the  $ET_0$  value for the RapidEye image (DOY 253) being 8% larger of that for the Landsat image (DOY 241). In relation to  $R_G$  and  $T_a$  these differences were also small for these days, 3% and 5%, respectively.

As there were no availability of images for both satellites in the same DOY, and with these small differences on the weather parameters, the Landsat Image (DOY 240) was normalized to the DOY 253 of the RapidEye, through  $R_G$  and  $T_a$  interpolated data, for respectively surface albedo ( $\alpha_0$ ) and surface temperature ( $T_0$ ). This allowed reasonable comparisons

between the results from the different spatial resolutions with similar thermohydrological conditions, by using  $ET_0$  data for DOY 253.

### 3.2 Remote sensing modeling input parameters

Fig. 2 shows the spatial distribution of the 24-hour  $\alpha_0$  values for the Landsat and RapidEye images in the mixed agro-ecosystems, during the driest period of the year 2011 inside the semi-arid reference study area of the Petrolina municipality, Pernambuco (PE) state, Northeast Brazil.

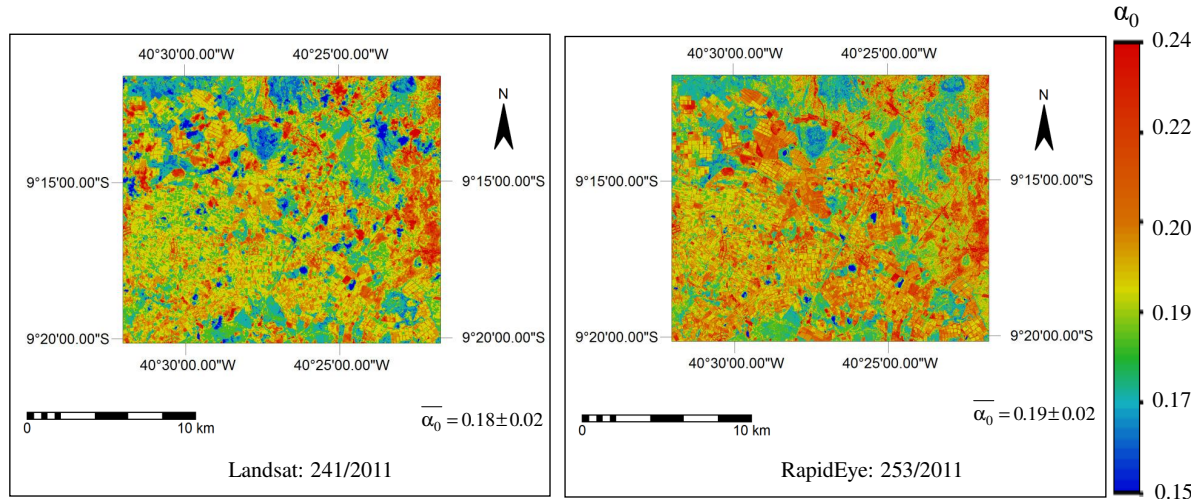


Figure 3. Spatial distribution of the 24-hour surface albedo ( $\alpha_0$ ) values for the Landsat and RapidEye images, during the driest period of the year 2011, in the semi-arid reference study area of Petrolina municipality, Pernambuco (PE) state, Northeast Brazil. The over bars means averages together with standard deviations.

The shortwave radiation balances among the different agro-ecosystems are strongly affected by  $\alpha_0$ . A darker surface presents low values, consequently has a higher available energy than a brighter one. It has been also reported that, besides the vegetation types and stages,  $\alpha_0$  depends on the soil moisture and crop management<sup>7-8</sup>. The bluish area in Fig. 3 represent the "Caatinga" species, which present low  $\alpha_0$  values, as they are darker than crops. Well-irrigated plots have lower  $\alpha_0$  than that for their drier surrounding areas. Then, as the highest average value is for the RapidEye image, and there is a large area under irrigation, as a first guess, the lower resolution of the Landsat over estimate irrigated areas. However, the  $\alpha_0$  spatial variations were homogeneous for both images with standard deviation (SD) of 0.02, with no strong distinctions among the mixed agro-ecosystems.

Values for  $\alpha_0$  were reported to be between 0.15 and 0.26, for tropical natural vegetation<sup>9</sup>, however the magnitudes in the current study are higher than those previously reported for humid tropical regions<sup>10-11</sup>, probably due to the high moisture conditions of these last climates. The relation of  $\alpha_0$  with environmental and moisture conditions is also in accordance with other more recent studies<sup>3,12-14</sup>.

The spatial distribution of the Normalized Difference Vegetation Index (NDVI) values for the Landsat and RapidEye images in the mixed agro-ecosystems inside the semi-arid reference study area of the Petrolina municipality, Pernambuco (PE) state, Northeast Brazil, are shown in Fig. 4.

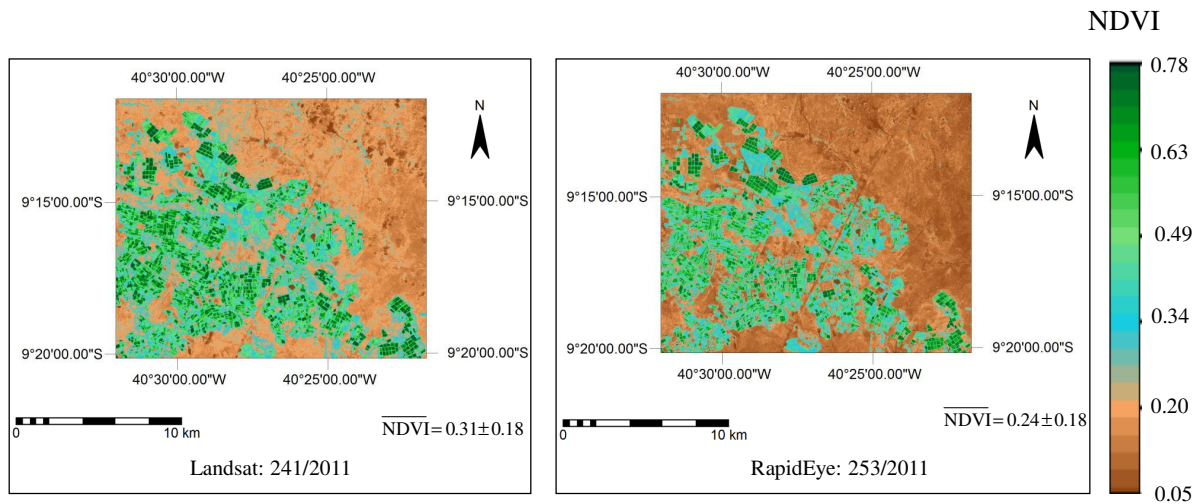


Figure 4. Spatial distribution the Normalized Difference Vegetation Index (NDVI) values for the Landsat and RapidEye images, during the driest period of the year 2011, in the semi-arid reference study area of Petrolina municipality, Pernambuco (PE) state, Northeast Brazil. The over bars means averages together with standard deviations.

In both satellite images, the distinctions of the NDVI values between irrigated crops and natural vegetation are much clear than in the case of  $\alpha_0$ , with the highest average for the Landsat satellite. Again, it is evidenced an overestimation of first ecosystem as crops produce under irrigation conditions much biomass than rainfed natural species during the driest period of the year, with the RapidEye mean pixel value being 77% of that for the Landsat image. As there is a relation between ET and NDVI<sup>15</sup>, the water fluxes will be higher for irrigated crops than for natural species, and these fluxes will be then overestimated in the Landsat results.

The spatial distribution of the 24-hour surface temperature ( $T_0$ ) values for the Landsat and RapidEye images in the mixed agro-ecosystems inside the semi-arid reference study area of the Petrolina municipality, Pernambuco (PE) state, Northeast Brazil, are presented in Fig. 5.

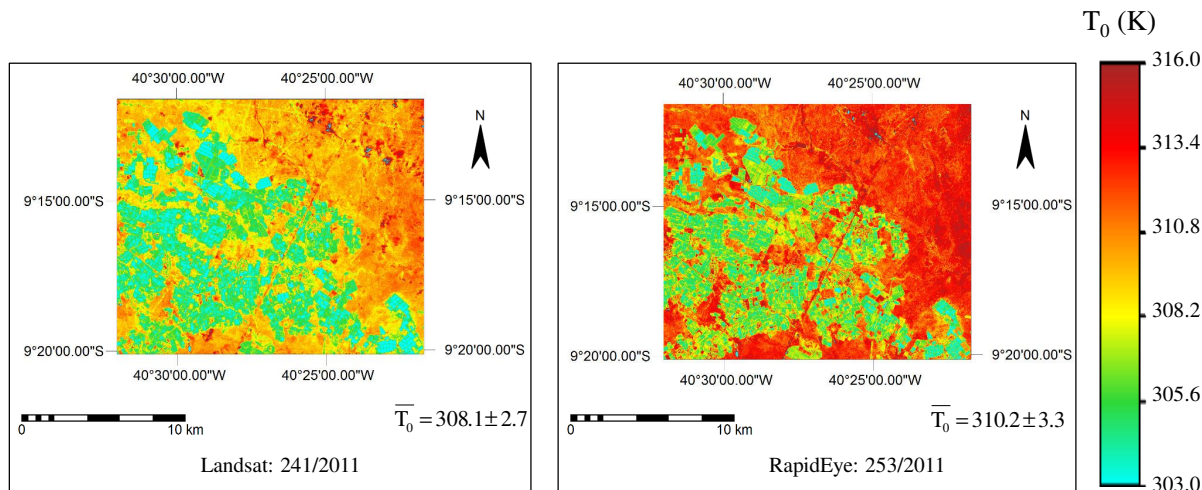


Figure 5. Spatial distribution the 24-hour surface temperature ( $T_0$ ) values for the Landsat and RapidEye images, during the driest period of the year 2011, in the semi-arid reference study area of Petrolina municipality, Pernambuco (PE) state, Northeast Brazil. The over bars means averages together with standard deviations.

$T_0$  affects the energy available, by interfering in the long wave radiation balance, with lower values under irrigation conditions than those for naturally drier areas. However, even differentiating the agro-ecosystems better than  $\alpha_0$  this distinction is not as strong as that for NDVI. One reason for this is the use of interpolated  $T_a$  and  $R_G$  data for retrieving  $T_0$  as residue in the radiation balance by Eq. 4. The lower average Landsat values are also explained by the over estimation of the irrigated area, as one can see by the larger and intense reddish colour in the RapidEye image with the average  $T_0$  pixel values being 1% higher than those for the Landsat image. These differences will affect ET and BIO results as consequences of different long wave emissions estimated by the two different satellite sensors.

Considering the mixed agro-ecosystems inside the whole study area, the frequency distribution for the modelling remote sensing input parameters are depicted in Fig. 6.

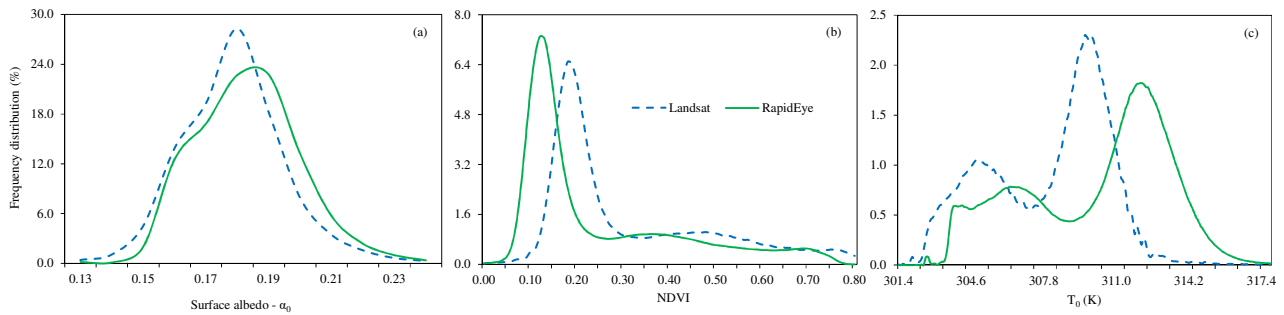


Figure 6. Frequency distribution of the modeling remote sensing input parameters for the Landsat and RapidEye images, during the driest period of the year 2011, in the semi-arid reference study area of Petrolina municipality, Pernambuco (PE) state, Northeast Brazil. (a) surface albedo -  $\alpha_0$ ; (b) Normalized Difference Vegetation Index - NDVI; surface temperature -  $T_0$ .

Considering  $\alpha_0$ , the value with the highest frequency were 0.19 (28%) and 0.20 (23%) for Landsat and RapidEye, respectively. For NDVI, they were 0.18 (6.5%) and 0.12 (7.3%), with the corresponding ones for  $T_0$  of 309.6 K (2.3%) and 312.1 K (1.8%). The different spatial resolutions between Landsat (30 m) and RapidEye (5 m), besides retrieving distinct average values for the modelling remote sensing parameters also will result in different frequency distribution curves. However, for both satellites, the  $\alpha_0$  curve, differently from the others, is symmetric, showing lower differences between irrigated crops and natural vegetation. The concentration of low NDVI values are for natural vegetation with the less high frequent values for irrigated crops; and clearly one can see two peaks for  $T_0$ , with the low values under irrigation conditions and the highest ones for the "Caatinga" species.

For both satellites, the spatial variability of  $\alpha_0$ , NDVI, and  $T_0$  in natural vegetation may be mainly attributed to variations in surface moisture conditions. However, for irrigated crops, as the water is in general regularly applied, the range of these remote sensing parameters are also influenced by different crop stages added by different irrigation and fertilization managements.

### 3.3 Retrieving water productivity components from Landsat image

To test the methodology from which  $T_0$  is retrieved by the residue in the radiation balance, giving confidence for using satellites without the thermal band, ET and BIO modelling results are compared with and without this band by processing the Landsat image (Fig. 7).

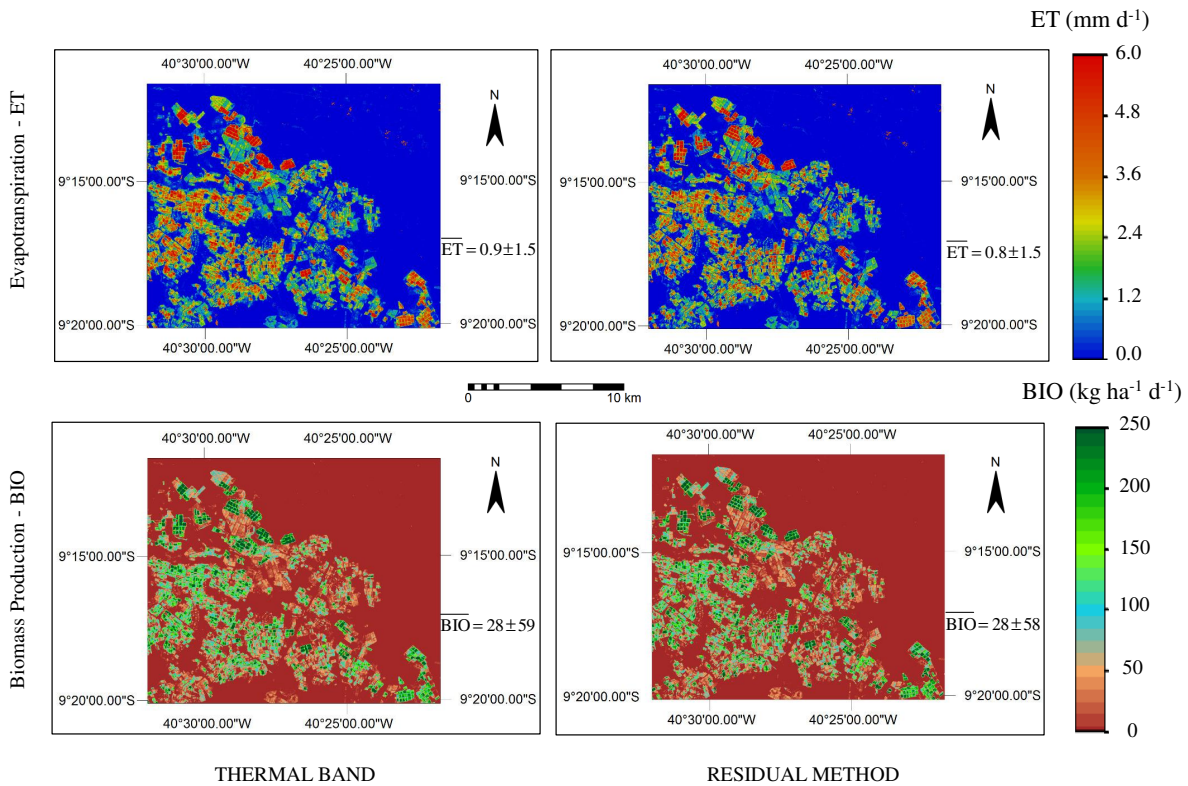


Figure 7. Spatial distribution of actual evapotranspiration (ET) and biomass production (BIO) by using both the Landsat thermal band and the residual method, during the driest period of the year 2011, in the semi-arid reference study area of Petrolina municipality, Pernambuco (PE) state, Northeast Brazil. The over bars means averages together with standard deviations.

From the one hand, when using the thermal band, its resolution of 100 m could affect the ET and BIO results. From the other hand, applying the residual method the interpolation of  $T_a$  and  $R_G$  will not translate very well the spatial surface characteristics. However, as  $\alpha_0$  and NDVI are involved in the residual  $T_0$  calculation, these effects are minimized.

The similarities of the results depicted in Fig. 7 resulting in mean WP (ET/BIO) of  $1.3 \pm 1.3 \text{ kg m}^{-3}$ , in both cases, by using or not the Landsat thermal band, are encouraging when having weather data availability, opening the opportunities for the use of high spatial and temporal resolution satellites without the thermal band, when aiming water productivity assessments. Both ET and BIO results from the Landsat image showed clearly the differences between "Caatinga" species with very low values, and the well-irrigated crops reaching to pixel values up to  $6 \text{ mm d}^{-1}$  and  $250 \text{ kg ha}^{-1} \text{ d}^{-1}$ , respectively, during this driest condition of the year in the Brazilian semi-arid region.

### 3.4 Water productivity assessments with RapidEye image

After having confidence on the residual method for retrieving  $T_0$ , the RapidEye image was tested for assessing WP by applying the SAFER algorithm together with the Monteith's Light Use Efficiency model - LUE (Fig. 8).

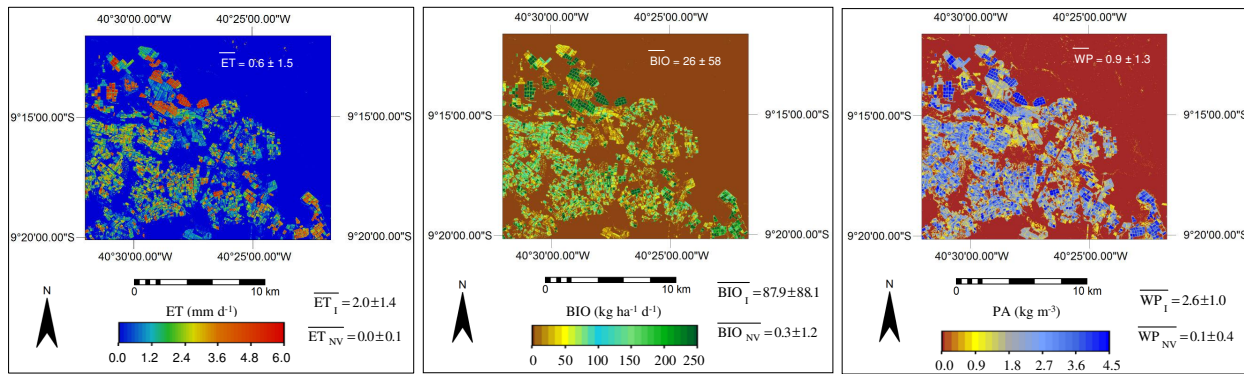


Figure 8. Spatial distribution of actual evapotranspiration (ET), biomass production (BIO) and water productivity (WP) by using the residual method on RapidEye image, during the driest period of the year 2011, in the semi-arid reference study area of Petrolina municipality, Pernambuco (PE) state, Northeast Brazil. The over bars means averages together with standard deviations, in Irrigated Crops (I) and Natural Vegetation (NV).

Comparing the ET and BIO results from the Landsat (Fig. 7) with those from RapidEye (Fig. 8) images, one can see that in the second one, the irrigated plots are more detailed, disregarding of using or not the Landsat thermal band. Spatial variations of these water productivity components with separation of irrigated crops (I) and natural conditions (NV), during the driest period of the year are evident. The ET and BIO high values, above 3.5 mm d<sup>-1</sup> and 150 kg ha<sup>-1</sup> d<sup>-1</sup>, respectively, are for the first ecosystem, composed by mainly grapes, mangoes, guavas and bananas, while "Caatinga" values for both parameters are close to zero, because of the largest fractions of the available energy being used as sensible heat flux (H) by the drier natural species. The ET and BIO ranges retrieve WP values for the NV and I ecosystems close to 0.0 and above 3.0 kg m<sup>-3</sup>, respectively. Stomata of "Caatinga" species close under these natural dryness conditions, limiting transpiration and photosynthesis, while; in general, fruit crops are daily irrigated based on their water requirements, reducing the heat losses to the atmosphere.

After applying the SUREAL model to the RapidEye WP results, it was verified that irrigated crops consumed  $2.0 \pm 1.3$  mm d<sup>-1</sup> more water than natural vegetation during the driest period in the Brazilian semi-arid region. In all agro-ecosystems, the plants are strongly sensitive to the spatial distribution of the soil water content, however, the higher standard deviation (SD) values for irrigated crops than for natural vegetation are mainly caused by different levels of fertilization, stages and irrigation management<sup>2</sup>.

As there is a relation between ET and BIO<sup>15</sup>, the BIO spatial variations are also strong during the climatically driest period of the year. Irrigation areas are well visible on the BIO map, confirming the effectiveness of coupling the SAFER and the Monteith LUE models with RapidEye images, with the irrigated crops producing  $88 \pm 87$  kg ha<sup>-1</sup> d<sup>-1</sup> more biomass than natural vegetation. For a completely growing season, irrigated corn crop showed twice the BIO values when comparing with natural alpine meadow in the Heihe River basin<sup>16</sup>, irrigation being considered the main reason for these differences.

Considering the WP incremental value during the natural driest condition of the study area, it was  $2.5 \pm 0.6$  kg m<sup>-3</sup>. Multiplying BIO by the Harvest Index (HI) makes it possible to estimate crop water productivity (CWP)<sup>17</sup>. The average crop coefficient ( $K_c$ ) values from field experiments were applied to reference evapotranspiration ( $ET_0$ ) and yield data by Teixeira and Bassoi<sup>18</sup> to estimate CWP in Petrolina-PE, resulting in 2.4, 1.5, 1.1 and 1.3 kg m<sup>-3</sup> for table grapes, mango, guava and banana crops, respectively. The mean CWP value of 1.8 kg m<sup>-3</sup> in this previous study give an HI of 0.70 when using the BIO results of the current research, which is also the average found for vineyards and mango orchards under the Brazilian semi-arid region by Teixeira et al.<sup>17</sup>, bringing confidence for the current RapidEye WP results.

#### 4. CONCLUSIONS

The SAFER algorithm was applied together with the Light Use Efficiency Monteith's model on Landsat and RapidEye satellite images having different spatial resolution by using and not using the Landsat thermal band. The Landsat image

was used to demonstrate the suitability of retrieving the water productivity components with a new methodology from which the surface temperature ( $T_0$ ) is estimated by residue in the radiation balance, allowing the use of high-resolution images which don't have this band. Comparing the Landsat results with and without the thermal bands there was no significant differences on the evapotranspiration (ET) and biomass production (BIO) values, what gave confidence for water productivity assessments by using RapidEye images. However, there were over estimations of irrigated areas when comparing the Landsat ET and BIO results with those derived from the RapidEye image due to more mixed pixels covered when using the first satellite. After applying the RapidEye images, the results indicated incremental values for water productivity (WP) of  $2.5 \pm 0.6 \text{ kg m}^{-3}$  during the driest conditions of the year 2011 in the Brazilian semi-arid region.

## ACKNOWLEDGEMENTS

The National Council for Scientific and Technological Development (CNPq) is acknowledged for the financial support to a project on Large-scale Water Productivity in Brazil.

## REFERENCES

- [1] Falkenmark, M., Rockström, J. Balance water for humans and nature. *Earthscan*, 2 ed., London, 247p (2005).
- [2] Claverie, M., Demarez, V., Duchemin, B., Hagolle, O., Ducrot, D., Marais-Sicre, C., Dejuoux, Jean-François, Huc, M., Keravec, P., Béziat, P., Fieuzaal, R., Ceschia, E. and Dedieu, G., "Maize and sunflower biomass estimation in southwest France using spatial and temporal resolution remote sensing data," *Remote Sens. Environ.* 124, 884-857 (2012).
- [3] Teixeira, A. H. de C. Hernandez, F. B. T., Warren, M. S., Andrade, R. G., Victoria, D. de C., Bolfe, E. L., Thenkabail, P. S. and Franco, R. A. M. Water Productivity Studies from Earth Observation Data: Characterization, Modeling, and Mapping Water Use and Water Productivity. In: Prasad, S.T. (Org). *Remote Sensing of Water Resources, Disasters, and Urban Studies*. 1ed.Boca Raton, Florida: Taylor and Francis, v. III, 101-126. (2015).
- [4] Chemin, B. J. and Alexandrisis, T., "Improving spatial resolution of ET seasonal for irrigated rice in Zhanghe, China," *Asian J. Geoinf.* 5, 3-11 (2004).
- [5] Allen, R. G., Pereira, L. S., Raes, D. and Smith, M., *Crop Evapotranspiration: Guidelines for Computing Crop Water Requirements*; Food and Agriculture Organization of the United Nations: Rome, Italy (1998).
- [6] Teixeira, A. H. de C., "Determination of surface resistance to evapotranspiration by remote sensing parameters in the semi-arid region of Brazil for land-use change analyses," IAHS Press, Wallingford, UK, 352, 167-170 (2012).
- [7] Teixeira, A. H. de C., Bastiaanssen, W. G. M., Ahmad, M-ud-D, Bos, M. G. and Moura, M. S. B., "Analysis of energy fluxes and vegetation-atmosphere parameters in irrigated and natural ecosystems of semi-arid Brazil," *J. Hydrol.* 362, 110-127 (2008).
- [8] Sandhu, H. S., Gilbert, R. A., Kingston, G., Subiros, J. F., Morgan, K., Rice, R. W., Baicum, L., Shine, J. M. and Davis, L., "Effects of sugarcane harvest method on microclimate in Florida and Costa Rica," *Agric. For. Met.* 177, 101-109 (2013).
- [9] Monteith, J. L. and Unsworth, M. H., *Principles of environmental physics*. Arnold: London, 291p., (1990).
- [10] Oguntoyinbo, J. S., "Reflection coefficient of natural vegetation, crops and urban surfaces in Nigeria," *Q. J. Roy. Meteor. Soc.* 96, 430-441, (1970).
- [11] Pinker, R. T., Thompson, O. E. and Eck, T. F., "The albedo of a tropical evergreen forest," *Q. J. Roy. Meteor. Soc.* 106, 551-558, (1980).
- [12] Lobell, D. B. and Asner, G. P., "Moisture effects on soil reflectance," *Soil Sci. Soc. Am. J.* 66, 722-727 (2002).
- [13] Li, S.-G., Eugster, W., Asanuma, J., Kotani, A., Davaa, G., Oyunbaatar, D. and Sugita, M., "Energy partitioning and its biophysical controls above a grazing steppe in central Mongolia," *Agric. For. Meteorol.* 137, 89-106 (2006).
- [14] van Dijk, A. I. J. M., Bruijnzeel, L. A. and Schellekens, J., "Micrometeorology and water use of mixed crops in upland West Java, Indonesia," *Agric. For. Meteorol.* 124, 31-49 (2004).
- [15] Yuan, M., Zhang, L., Gou, F., Su, Z., Spiertz, J. H. J., Werf, W. van der., "Assessment of crop growth and water productivity for five C3 species in the semi-arid Inner Mongolia," *Agric. Water Manage.* 122, 28-38 (2013).

- [16] Wang, Ma, M., Huang, G., Veroustraete, F., Zhang, Z., Song, Y. and Tan, J, "Vegetation primary production estimation at maize and alpine meadow over the Heihe River Basin, China," *Int. J. Appl. Earth Obs. Geoinf.* 17, 94-101 (2012).
- [17] Teixeira, A. H. de C., Bastiaanssen, W. G. M., Ahmad, M-ud-D and Bos, M. G., "Reviewing SEBAL input parameters for assessing evapotranspiration and water productivity for the Low-Middle São Francisco River basin, Brazil Part B: Application to the large scale, " *Agric. For. Meteorol.* 149, 477-490 (2009).
- [18] Teixeira, A. H. de C. and Bassoi, L. H., "Crop Water Productivity in Semi-arid Regions: From Field to Large Scales," *Ann. Arid Zone*, 48, 1-13 (2009).